International Journal of Control and Automation
Vol.8, No.10 (2015), pp.237-250
http://dx.doi.org/10.14257/ijca.2015.8.10.23

Online Detection System for Inner Leakage Failure of Heater

Wang Xin-hua[1, 2], Jiao Yu-lin[2], Niu Yong-chao[3] and Yang Jie[2]

[1.] *Shangqiu Vocational and Technical College, Shangqiu 476000, China*
[2.] *Wuhan University of Technology, Wuhan 430063, China;*
[3.] *Shangqiu Jinpeng Industrial Co., Ltd., Shangqiu 476000, China*
gyxxwxh@163.com

Abstract

The present study, based on the modular and graphical LabVIEW development platform, is dedicated to developing the online detection system for inner leakage failure of heater, in order to complete the online detection and the quantitative diagnosis of the inner leakage failure of the high-pressure and temperature heater in the power plant, and finally apply the system to engineering practice. With this purpose, this study produces some innovative designs in light of the structure and working principles of the online detection system, analyzes and selects the hardware modeling, assesses and designs the key modules and finally analyzes and verifies the implementation and performance of the system. At last, this paper concludes that the online detection system performs well in filtering, and functions accurately and reliably in processing signals.

Keywords: *Acoustic Emission, High-Pressure Heater, Leakage, Online Detection, Acoustic Emission Signals*

1. Introduction

The function of the online leakage detection system of high-pressure heater is shown in Figure 1:

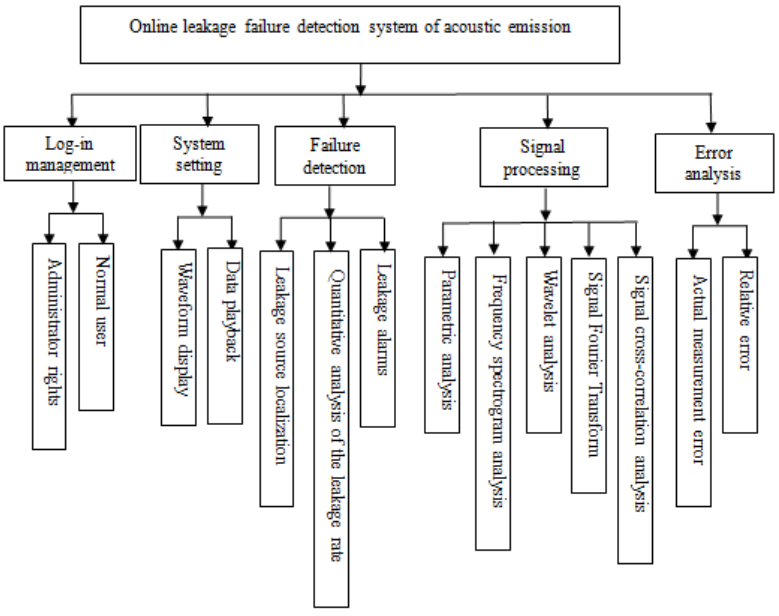

Figure 1. Functions of Online Leakage Detection System of High-Pressure Heater

ISSN: 2005-4297 IJCA

According to the signal flow, the software system can be divided into four modules: signal collection, signal analysis, signal storage and signal playback. The signal firstly travels through the first module and then is processed by the analysis and storage modules at the same time. Finally, the result of the analysis is displayed. The structure of the system is shown in Figure 2.

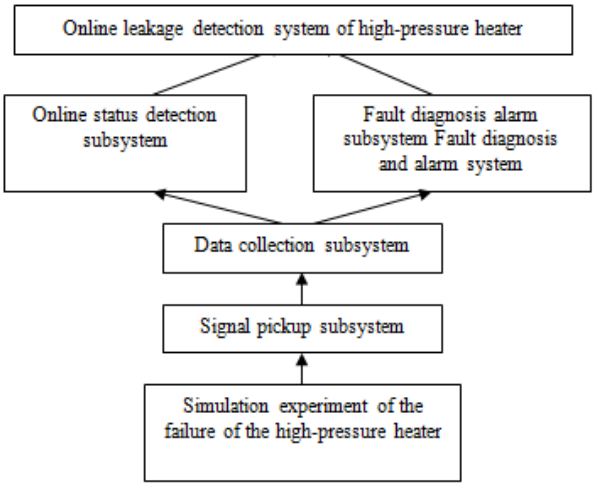

Figure 2. Overall Structure of the System

The main interface of the online detection system is shown in Figure 3. To ensure the system is in safe operation, it has differentiated designs for users with different rights: only users with certain rights can register for enjoying certain functions. When the system starts working, the user of technology can set their user password and right in the setup menu. On the left of the main interface are the warning light indicator, the function button control area and the display instrument of rotation rate and noise. On the right is the function display area including the time-domain graph, the frequency spectrogram, the single-channel history graph, the vibration mode analysis chart, the failure detection area, the real-time data display area and the alarm data display area.

Figure 3. Main Interface of the System

2. Key Module Design

Key module design includes filtering module design, signal analysis module design, condition monitoring module design, detection module design for leakage

failure, error analysis module design, module design for signal storage and data access, and FFT module design.

(1) Detection module design for leakage failure

The principle of designing the leakage failure detection program is to extract center frequency after the leakage signal undergoes filtering and FFT. If the peak frequency ranges from 30 kHz to 40 kHz, there is leakage failure. Figure 4 shows the procedure of the leakage failure detection.

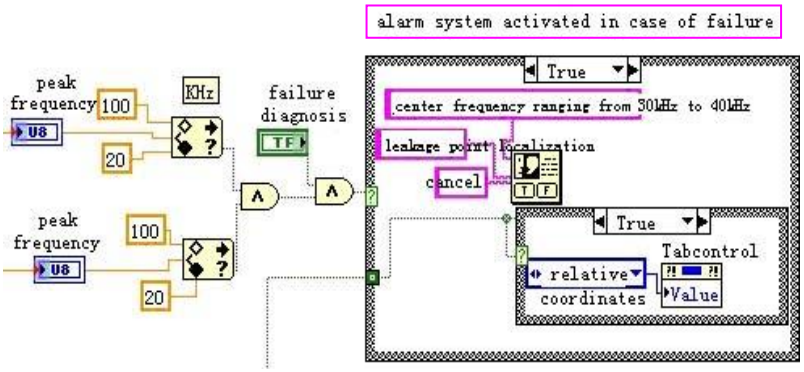

Figure 4. Flow Chart of the Leakage Failure Detection

(2) Error analysis module design

The function of error calculation is fulfilled by the sub-template in the LabVIEW functions palette. Figure 5 is the flow chart of the procedure.

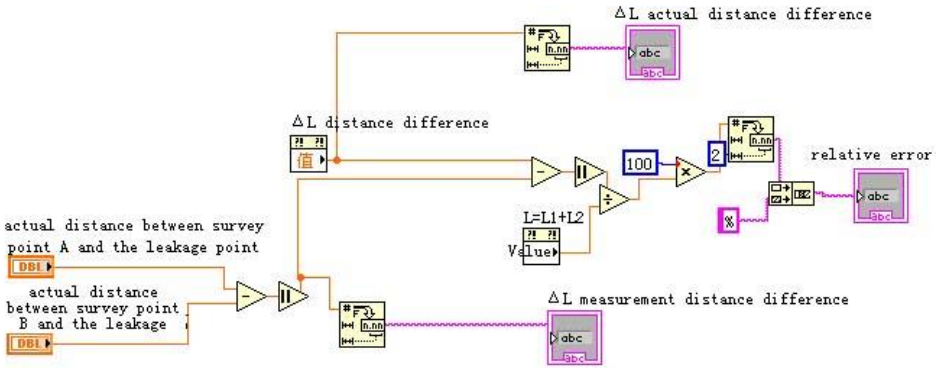

Figure 5. The Flow Chart of the Error Calculation

(3) Module design for signal storage and data access

The signal is stored in the text file format with .txt being the suffix of the filename. In order to distinguish the stored signals, the file is named after the system time when the computer is collecting signals. The signal is automatically stored in a default file every time signal collection is finished. The storage process is shown in Figure 6.

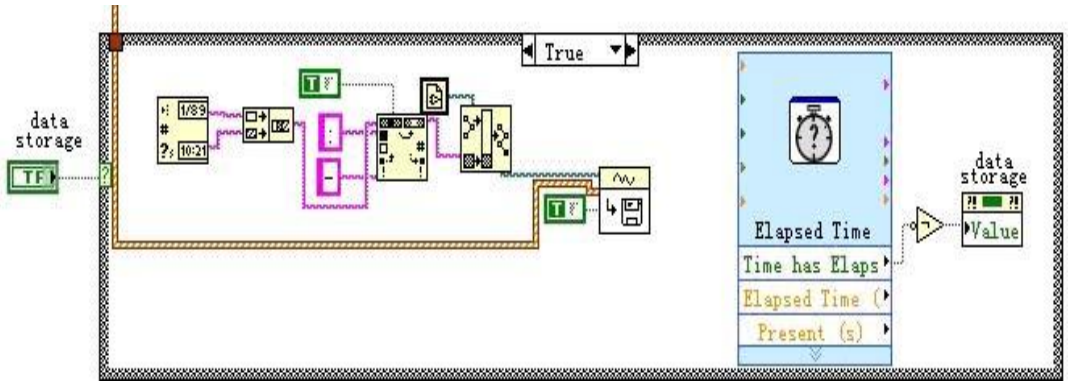

Figure 6. The Flow Chart of Signal Storage

(4) FFT module design

The present study uses the FFT transformed cross-correlation function and LabVIEW program to do the cross-correlation analysis of the leakage signal in the internal pipeline of the heater. In this way, this paper can get transition time τ and locate the leakage points in the high-pressure heaters.

First of all, the acoustic emission signals collected from the dual channels undergo filtering and FFT. Then the curve of the correlation analysis is obtained. Finally, use the peak points of the curve and their locations to obtain transition time τ. The process is illustrated in Figure 7.

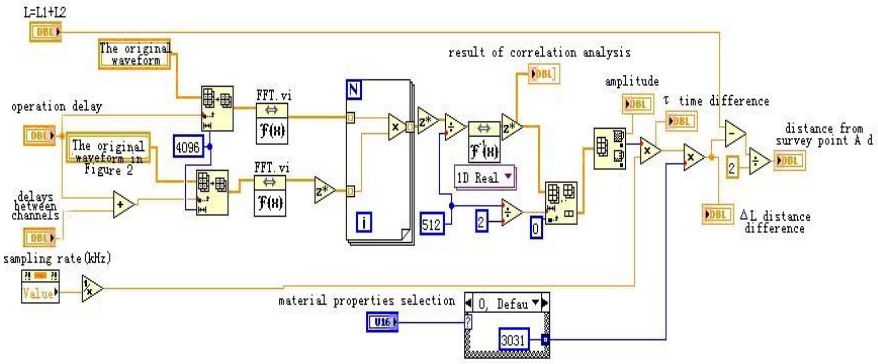

Figure 7. Flow Chart of the Correlation Analysis

3. System Performance

(1) Signal collection

Programming enables the computer to read signals from the acquisition cards and put the signal data in a pre-allocated memory for further processing. The parameter most relevant to data collection is sampling rate f_s, the number of data points collected by the acquisition cards per minute; another most relevant parameter is n_s, the number of data points read from the cards by the computer every time. The two are different because f_s is a parameter used for data collection performed by the acquisition cards and is influenced by the performance of the cards, while n_s is influenced by the computer. Also, the value of n_s is related to that of f_s. Normally, the former is 1/2 to 1/4 of that of the

latter so that the data can be updated two to four times per minute, which makes it convenient to observe their change. The improperly large value is inclined to make the computer run out of memory [1-5]. The structure of data collection is shown in figure 8.

The development of the collection module consists of three steps.

(a) Create a collection task. Choose a physical channel; appoint the type of the collection parameters (including voltage, electric current, temperature, etc.). And name the task;

(b) Set the parameters. This includes setting sampling rate f_s, sampling mode and the signal range (which is related to precision);

Start signal collection and access. After the collection is started, signal access VI keeps accessing data until the system gives the order to stop.

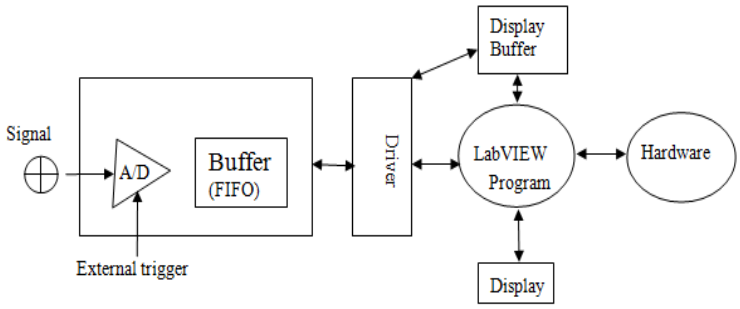

Figure 8. Structure of Data Collection

Figure 9 is the flow chart of the signal collection system. Signal collection can be carried out when the sampling of the censor is set up correctly. When the set-up module is completed, the related sampling parameters are input to collection module to help fulfill signal collection.

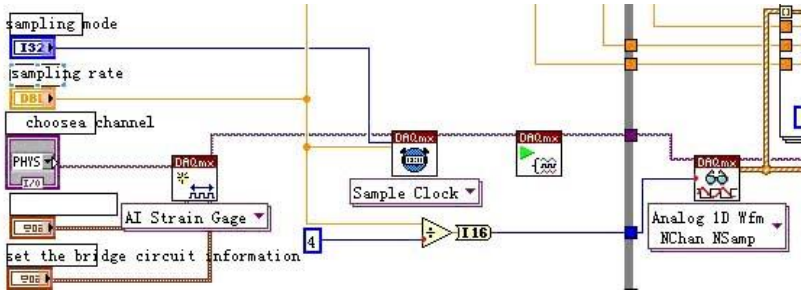

Figure 9. Flow Chart of the Collection Module System

(2) Signal analysis processing

Signal analysis processing module is made up of the real-time data display part, the alarm zone, the real-time curve display part, modal analysis part, etc.

There are two ways to carry out modal analysis. One is to use the method of multi-points adjustment incentive to directly get the "pure modal" of the system as well as related parameters; the other method is to find out the "frequency response function "between the incentive points and the survey points through the single-point incentive. Then it establishes the frequency response function matrix to perform analysis and obtain the modal shape in each order as well as the related modal parameters. This paper applies the second method to carry out modal analysis. The physical significance of the frequency response function lies in the response of point *i* provoked by the unit force exerted on

point *j*. This paper deduces the response formula from past literature [6-10] which is shown below.

$$\{X\}=\sum_{r=1}^{N}\frac{\{\varphi_r\}\{\varphi_r\}^T\{F\}}{k_r\left[1-\left(\frac{\omega}{\Omega_r}\right)^2+j2\zeta_r\left(\frac{\omega}{\Omega_r}\right)\right]},\ \Omega_r=\sqrt{k_r/m_r} \tag{1}$$

In the formula above, $\{\varphi_r\}$ represents the r order modal shape matrix; $\{F\}$ is excitation force, k_r is stiffness; ζ is damping ratio; Ω_r is r order natural frequency. If $\lambda_r=\omega/\Omega_r$, then

$$\{X\}=\sum_{r=1}^{N}\frac{\{\varphi_r\}\{\varphi_r\}^T\{F\}}{k_r\left(1-\lambda_r^2+j2\zeta_r\lambda\right)} \tag{2}$$

Suppose the excitation force F_j is only exerted on point *j* in the structure, then

$$\{F\}=\begin{Bmatrix}0 & 0 & \cdots & F_j & 0 & \cdots & 0\end{Bmatrix}^T \tag{3}$$

Therefore,

$$\frac{X_i}{F_j}=\sum_{r=1}^{N}\frac{\{\varphi_r\}\{\varphi_r\}^T}{k_r\left(1-\lambda_r^2+j2\zeta_r\lambda\right)} \tag{4}$$

Based on the definition, the frequency response function is:

$$H_{ij}(\omega)=\frac{X_i}{F_j}=\sum_{r=1}^{N}\frac{\{\varphi_r\}\{\varphi_r\}^T}{k_r\left(1-\lambda_r^2+j2\zeta_r\lambda\right)} \tag{5}$$

If $[F]=[F_1 \quad F_2 \quad \cdots \quad F_N]^T$, according to linear superposition principle, there should be

$$X_i=H_{i1}F_1+H_{i2}F_2+\cdots+H_{iN}F_N=\begin{bmatrix}H_{i1} & H_{i2} & \cdots & H_{iN}\end{bmatrix}\begin{Bmatrix}F_1\\F_2\\\vdots\\F_N\end{Bmatrix} \tag{6}$$

Also,

$$[X]=[H]\{F\} \tag{7}$$

Therefore,

$$[H]=\sum_{r=1}^{N}\frac{\{\varphi_r\}\{\varphi_r\}^T}{k_r\left(1-\lambda_r^2+j2\zeta_r\lambda\right)} \tag{8}$$

Expand formula (8) and get formula (9):

$$[H]=\sum_{r=1}^{N}[{}_{r}H]=\sum_{r=1}^{N}\frac{1}{k_r\left(1-\lambda_r^2+j2\zeta_r\lambda\right)}\left[\begin{Bmatrix}\varphi_{1r}\\ \varphi_{2r}\\ \vdots\\ \varphi_{Nr}\end{Bmatrix}\begin{bmatrix}\varphi_{1r} & \varphi_{2r} & \cdots & \varphi_{Nr}\end{bmatrix}\right] \quad (9)$$

Given $Y_r=\frac{1}{k_r\left(1-\lambda_r^2+j2\zeta_r\lambda\right)}$, then (9) can be further transformed to

$$[H]=\sum_{r=1}^{N}[{}_{r}H]=\sum_{r=1}^{N}Y_r\begin{bmatrix}\{\varphi_r\}\varphi_{1r} & \{\varphi_r\}\varphi_{2r} & \cdots & \{\varphi_r\}\varphi_{Nr}\end{bmatrix} \quad (10)$$

In (10), $[{}_{r}H]$ stands for the contribution made by r order mode to $[H]$ and thus can be called the frequency response function matrix of r order mode. Therefore, two results can be achieved:

a) Any column in the frequency response function matrix is:

$$\begin{aligned}\begin{bmatrix}H_{i1} & H_{i2} & \cdots & H_{iN}\end{bmatrix}&=\sum_{r=1}^{N}Y_r\left[\varphi_{ir}\{\varphi_r\}^T\right]=\sum_{r=1}^{N}\begin{bmatrix}{}_{r}H_{i1} & {}_{r}H_{i2} & \cdots & {}_{r}H_{iN}\end{bmatrix}\\&=\sum_{r=1}^{N}Y_r\varphi_{ir}\begin{bmatrix}\varphi_{1r} & \varphi_{2r} & \cdots & \varphi_{Nr}\end{bmatrix}\\&=\frac{\varphi_{ir}}{k_r\left(1-\lambda_r^2+j2\zeta_r\lambda\right)}\begin{bmatrix}\varphi_{1r} & \varphi_{2r} & \cdots & \varphi_{Nr}\end{bmatrix}\end{aligned} \quad (11)$$

In (11), any column in $[H]$ includes all modal parameters. The ratio of the frequency response function values of the r order mode in the above-mentioned column is the r order modal shape. This result shows that if vibration pickup is done in a fixed point i in the structure and all other points are excited alternately, one column of $[H]$ can be obtained. The frequency response function in this column can involve all information necessary for making modal analysis.

b) Any row in the frequency response function matrix is:

$$\begin{Bmatrix}H_{1j}\\ H_{2j}\\ \vdots\\ H_{Nj}\end{Bmatrix}=\sum_{r=1}^{N}\begin{Bmatrix}{}_{r}H_{1j}\\ {}_{r}H_{2j}\\ \vdots\\ {}_{r}H_{Nj}\end{Bmatrix}=\sum_{r=1}^{N}Y_r\begin{Bmatrix}\varphi_{1r}\\ \varphi_{2r}\\ \vdots\\ \varphi_{Nr}\end{Bmatrix}\varphi_{jr}=\sum_{r=1}^{N}\frac{\varphi_{ir}}{k_r\left(1-\lambda_r^2+j2\zeta_r\lambda\right)}\begin{Bmatrix}\varphi_{1r}\\ \varphi_{2r}\\ \vdots\\ \varphi_{Nr}\end{Bmatrix} \quad (12)$$

(12) Reflects that any row in $[H]$ contains all modal parameters. And the ratio of the r modal frequency response function in the row is the r order modal shape shown in (13):

$$\begin{Bmatrix}\varphi_{1r}\\ \varphi_{2r}\\ \vdots\\ \varphi_{Nr}\end{Bmatrix}=\frac{1}{Y_r\varphi_{jr}}\begin{Bmatrix}{}_{r}H_{1j}\\ {}_{r}H_{2j}\\ \vdots\\ {}_{r}H_{Nj}\end{Bmatrix} \quad (13)$$

This proves that if vibration is excited in a fixed point j and picked up in all other points, then a row of the frequency response function matrix is obtained. Such row in the frequency response function can involve all information necessary for modal analysis.

Based on the resolution principles of the frequency response function and using MP_FRF synthesis and MP_FDPI analytic function, the system obtains the information of the frequency response function illustrated in Figure 10.

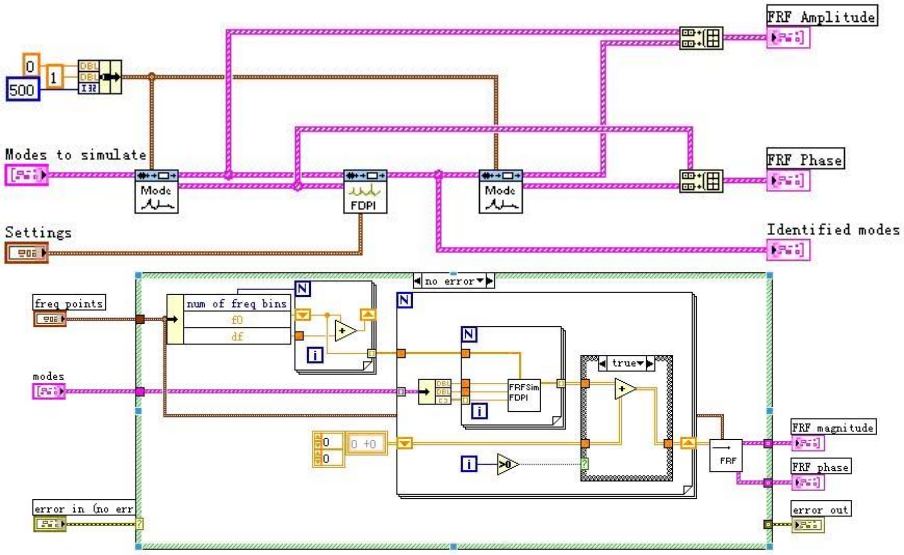

Figure10. Resolution of the Frequency Response Function

The modal analysis part of this system is a program of the modal analysis in the dynamical property analysis. It reflects real-time modal changes of the whole pipeline vibration after its wall starts vibrating. Figure 11 illustrates the modal analysis.

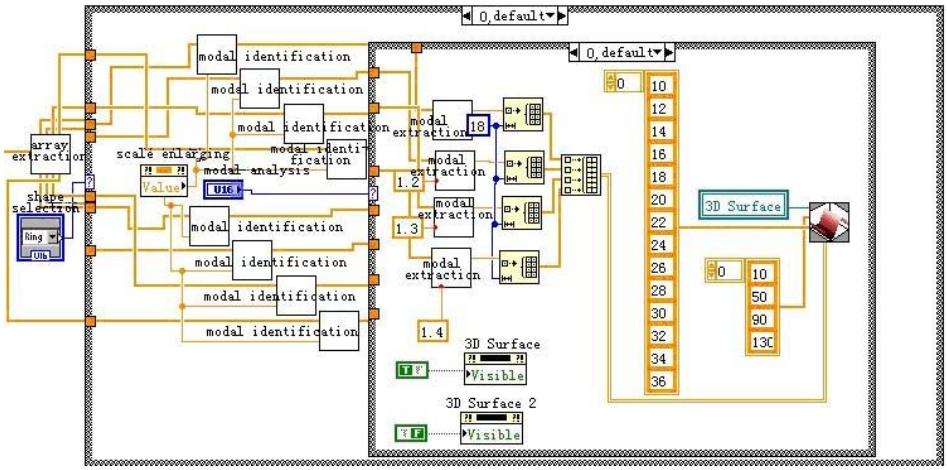

Figure11. The Flow Chart of the Modal Analysis

4. System Performance Test

To test the accuracy and reliability of the leakage failure detection system of heater, the present study takes the PCI-2acoustic emission detection system as reference, and uses the two systems to conduct comparison experiments of the high-pressure heater leakage failure under the leakage conditions in the test bench. The PCI-2acoustic emission detector, produced in America, is a world renowned acoustic emission signals detector with high detection precision and reliable data. If the results gained by the system developed by the present study are largely different from that achieved by the PCI-2acoustic emission detection system, the former system should be adjusted and improved

until its results are similar to the referred ones. If the results drawn by the two systems are basically the same, the leakage failure detection system of heater performs accurately and reliably.

Test method

The plan of system performance test consists of two parts:

Test of signal processing function

Because the hardware may exert certain influence on data collection, the study takes the experimental data acquired by PCI-2acoustic emission detection system under different leakage conditions as the standards to test the reliability and accuracy of the signal processing function of the leakage failure detection system of heater.

test of overall system performance

The present study uses the two systems to test the acoustic emission signals sent by the tested heater under different leakage conditions, and also measures and records the time and amount of the leakage under each condition. Then, it analyzes and compares two changing curves of the feature parameters of acoustic emission signal of leakage over different pressures gained by two systems. In this way, the sensitivity of the leakage failure detection system is tested. For the precision and accuracy of the quantitative detection of the system, the study calculates and analyzes the error between the standard leakage rate and the actual leakage rate.

5. Verification of the Signal Processing Performance Test

In this part, the paper takes the analyzed results of the acoustic emission signals under different working conditions as a case study, to verify the performance superiority of the leakage failure detection system of heater.

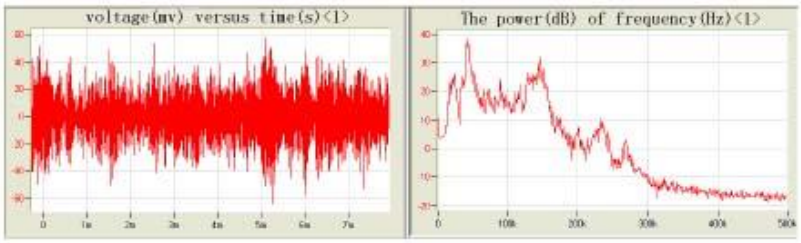

A) PCI-2test Result of Acoustic Emission Detection System

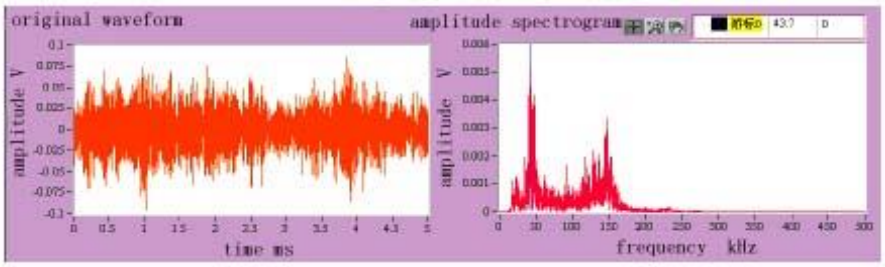

B) Test Result of Leakage Failure Detection System of Heater

Figure 12. Time-Domain Waveform and Frequency Spectrogram of Acoustic Emission Signal of Leakage When the Leak Is 1mm in Diameter and Pressure Is 0.3mpa

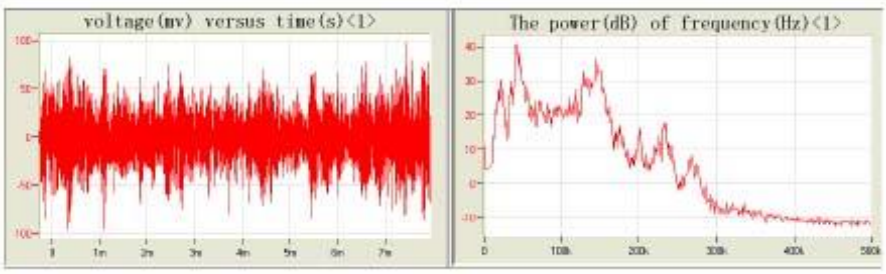

A) PCI-2test Result of Acoustic Emission Detection System

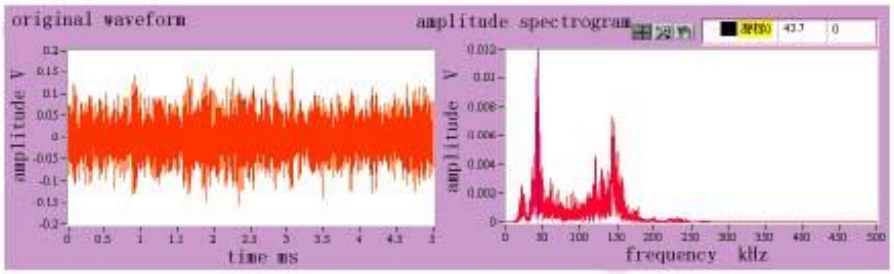

B) Test Result of Leakage Failure Detection System of Heater

Figure 13. Time-Domain Waveform and Frequency Spectrogram of Acoustic Emission Signal of Leakage when the Leak is 1mm in Diameter and Pressure is 0.6mpa

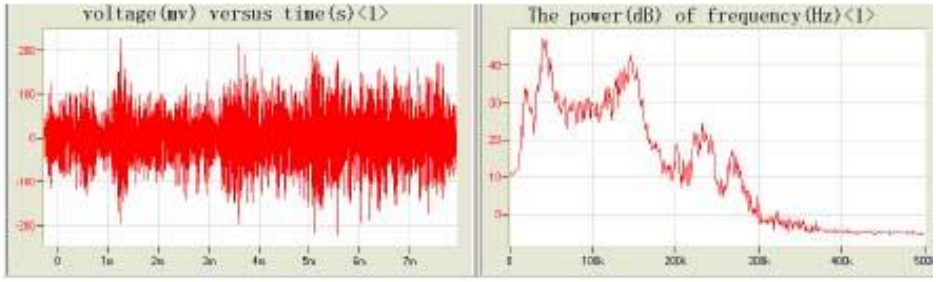

A) Pci-2 Test Result of Acoustic Emission Detection System

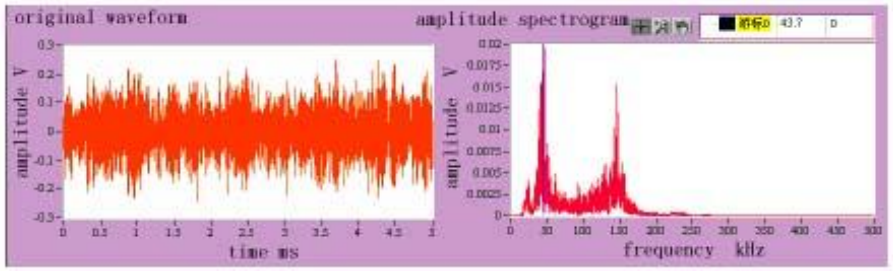

B) Test Result of Leakage Failure Detection System of Heater

Figure 14. Time-Domain Waveform and Frequency Spectrogram of Acoustic Emission Signal of Leakage when the Leak is 1mm in Diameter and Pressure is 0.9mpa

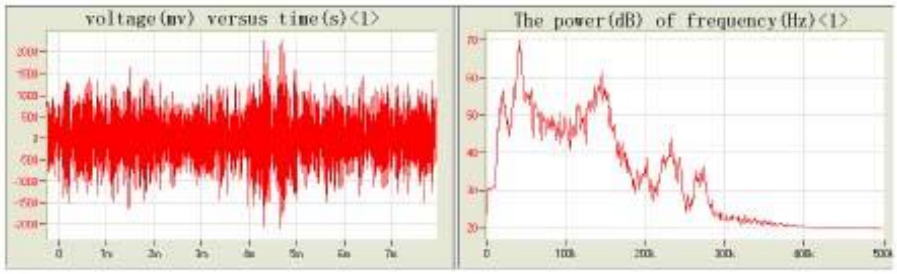

A) PCI-2test Result of Acoustic Emission Detection System

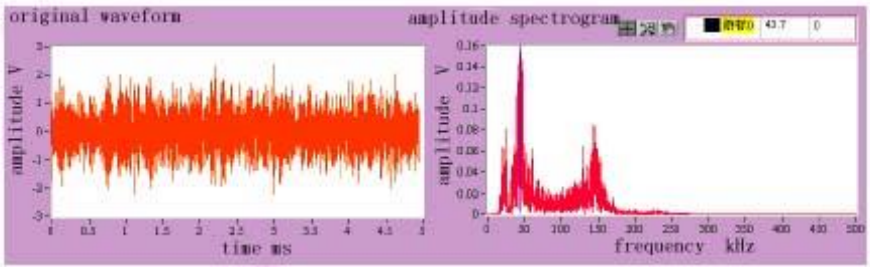

B) Test Result of Leakage Failure Detection System of Heater

Figure 15. Time-Domain Waveform and Frequency Spectrogram of Acoustic Emission Signal of Leakage when the Leak is 2mm in Diameter and Pressure is 0.6mpa

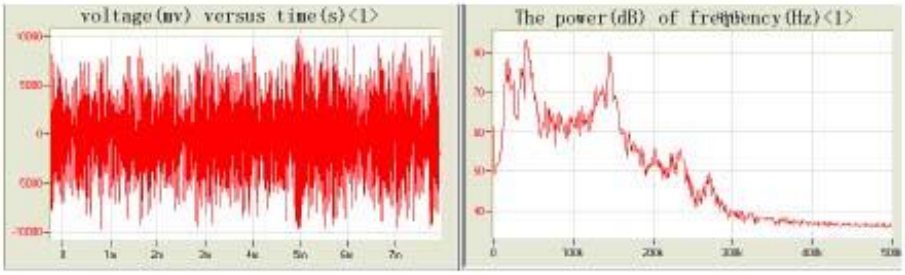

A) PCI-2test Result of Acoustic Emission Detection System

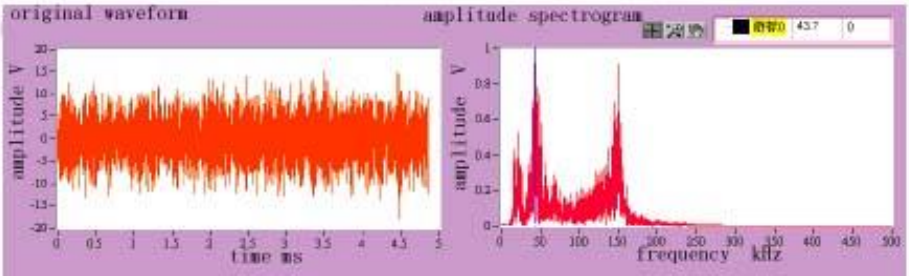

B) Test Result of Leakage Failure Detection System Of Heater

Figure 16. Time-Domain Waveform and Frequency Spectrogram of Acoustic Emission Signal of Leakage when the Leak is 2mm in Diameter and Pressure is 0.6mpa

Figure 12 - 16 prove that the amplitudes of the time-domain waveforms and frequency spectrograms of the two systems increase as the leak and the pressure grow. When the leaks and pressures of the two systems are the same, the amplitudes of the time-domain waveforms have the same orders of magnitude. As for frequency domain, the heater acoustic emission signals of leakage in both systems have peaks near 40kHz and 150kHz

respectively, and distribute between 32kz~60kHz and 135kHz ~170kHz respectively. The sizes of the two peaks increase as the leak and pressure grow but are basic the same. Furthermore, by comparing the two systems, this paper finds that PCI-2acoustic emission detection system cannot eliminate the unwanted signals effectively because there are always two to three peaks near 200kHz~300kHz which are noise signals according to literature records and theoretical analysis. However, the leakage failure detection system of heater can effectively eliminate these signals. Therefore, its software system has strong filtering capability and acts accurately and reliably in signal processing.

6. Conclusion

By taking the experimental data acquired by PCI-2acoustic emission detection system under different leakage conditions as the standards and comparing them with the results produced by the system developed by the present study, this paper concludes that the leakage failure detection system of heater can eliminate noise in the environment effectively, and analyze and process the acoustic emission signal of leakage accurately.

Acknowledgements

Foundation item: Nature Science Foundation of Henan Science and Technology Bureau (141008) (141080); Major science and technology research plan project in Henan province (142102110028);

References

[1] G. Cammarata, L. Monaco, L. Cammarata and G. Petrone, "A numerical procedure for pcm thermal storage design in solar plants[J]", International Journal of Heat and Technology, Volume 31, No 2 **(2013)**, Pages105-110.
[2] G. Heo and S.K. Lee, "Internal leakage detection for feedwater haters in power plants using neural networks[J]", Expert Systems with Applications, Volume 39, Issue 5, April 2012, Pages 5078-5086.
[3] M.J. Eaton, R. Pullin, K.M. Holford, "Acoustic emission source location in composite materials using Delta T Mapping[J]", Composites Part A: Applied Science and Manufacturing, Volume 43, Issue 6, June 2012, Pages 856-863
[4] S. Hao, J. Shuguang, W. Lanyun and W. Zhengyan, "King factor of the strata overlying the gob and a three-dimensional numerical simulation of the air leakage flow field[J]", Mining Science and Technology (China), Volume 21, Issue 2, March 2011, Pages 261-266
[5] W.M. Chambers and N.J.McC. Mortensen, "Toperative leakage and abscess formation after colorectal surgery[J]", Best Practice & Research Clinical Gastroenterology, Volume 18, Issue 5, October 2004, Pages 865-880.
[6] C.M. Keum, J.H. Bae, M.H. Kim, W. Choi and S.D. Lee, "Ution-processed low leakage organic field-effect transistors with self-pattern registration based on patterned dielectric barrier[J]", Organic Electronics, Volume 13, Issue 5, May 2012, Pages 778-783.
[7] M. Cucumo, V. Ferraro, D. Kaliakatsos and V. Marinelli, "A calculation model for a thermodynamic analysis of solar plants with parabolic collectors cooled by air evolving in an open joule-brayton cycle[J]", International Journal of Heat and Technology, Volume 31, No 2 (2013), Pages127-134.
[8] H. Román-Flores, A. Flores-Franulič and Y. Chalco-Cano, "fuzzy integrals[J]", Applied Mathematics and Computation, Volume 204, Issue 1, 1 October 2008, Pages 178-183.
[9] Lei, Cuihong ,Zou and Pinghua, "Application of neural network in heating network leakage fault diagnosis [J]", Journal of Southeast University. v 26, n 2, p 173-176, 2010.
[10] Zhou, H. Donghua, H. Xiao, W. Zidong, L. Guo-Ping and J. D. Yindong, "Leakage Fault Diagnosis for an Internet-Based Three-Tank System: An Experimental Study", IEEE Transactions on Control Systems Technology, June 13, 2011[C].
[11] Ergün Tuncay and Yuzo Obara, "Comparison of stresses obtained from Acoustic emission and Compact Conical-Ended Borehole Overcoring techniques and an evaluation of the Kaiser Effect level[J]', Bulletin of Engineering Geology and the Environment, 2012, Volume 71, Number 2, Pages 367-377.
[12] Q. Dai, K. Ng, J. Zhou, E.L. Kreiger and T.M. Ahlborn, "Damage investigation of single-edge notched beam tests with normal strength concrete and ultra-high performance concrete specimens using acoustic emission techniques[J]", Construction and Building Materials, Volume 31, June 2012, Pages 231-242.

[13] D. De Wrachien, G. Lorenzini and M. Medici, "water droplet and aerial path in irrigation systems: classical and quantum termofluidynamical approaches and numerical approximation methods [J]", International Journal of Heat and Technology, Volume 31 No 2 **(2013)**, Pages81-86.